

## **Supplemental data**

### **Materials and Methods**

#### **VLS-101 generation**

VLS-101 comprises the ROR1 targeting antibody, UC-961, a proteolytically cleavable maleimidocaproyl-valine-citrulline-para-aminobenzoate (mc-vc-PAB) linker, and the anti-microtubule cytotoxic agent MMAE (Figure 1A). Briefly, UC-961 was diluted (44 mg/mL in 50 mM sodium citrate, 10 mg/mL trehalose, 0.05 mM ethylenediaminetetraacetic acid (EDTA), 0.02% polysorbate 80, pH 5.2) and pH-adjusted by the addition of 33% v/v (of starting antibody volume) 500 mM Tris-Cl, 25 mM EDTA, pH 8.0 to target a concentration of approximately 33 mg/mL and a pH of 8. 10 mM tris(2-carboxyethyl)phosphine in water was added to achieve 2 equivalents per antibody and UC-961 was reduced for 90 minutes at 20°C to generate approximately four free thiols. The partially reduced UC-961 was diluted to approximately 10 mg/mL with 25 mM Tris-Cl, 150 mM NaCl, pH 8.0 before conjugation with mc-vc-PAB-MMAE. 10 mM mc-vc-PAB-MMAE in dimethylacetamide (DMA) was added to 5 equivalents (with additional DMA added to achieve 5% v/v DMA during conjugation) and the conjugation reaction was allowed to proceed for 60 minutes at 20°C. 10 mM N-acetyl cysteine in water was then added to quench excess mc-vc-PAB-MMAE. The quench reaction was allowed to proceed for 60 minutes at 20°C before the conjugate was purified and formulated by buffer exchange into 25 mM His/Cl, 200mM sucrose, 0.01% w/v PS20 using gravity G25 columns. The purified ADC was analysed by ultraviolet spectroscopy, hydrophobic interaction chromatography (HIC), and size-exclusion chromatography (SEC) to determine the protein concentration, drug-to-antibody ratio (DAR), and monomer/dimer content, respectively.

#### **VLS-101 cellular binding**

A binding assay of the naked antibody (UC-961) and the ADC (VLS-101) to ROR1-positive mantle cell lymphoma (MCL; JeKo-1) cell line and primary CLL cells purified from different patients was performed.  $0.5 \times 10^6$  cells were plated in 50  $\mu\text{L}$  on each well of a 96-well deep-well plate (ThermoFisher Scientific #249946, Waltham, MA). A 1:3 dilution series of UC-961 was made starting with 2  $\mu\text{g}/\text{mL}$  starting stock. Thereafter, 50  $\mu\text{L}$  of different concentrations of UC-961 (from 17  $\text{pg}/\text{mL}$  to 1000  $\text{ng}/\text{mL}$  final concentration) were added. Cells and antibody were mixed and incubated on ice for 20 minutes. Samples were then washed twice with fluorescent-activated cell sorter (FACS) buffer and, after the second wash, cells were resuspended in 100  $\mu\text{L}$  of anti-human IgG secondary phycoerythrin (PE) antibodies (ThermoFisher Scientific #124998-82, Waltham, MA) at 1  $\mu\text{g}/\text{mL}$  final concentration and incubated on ice (in the dark) for 20 minutes. Cells were washed twice as described previously and analyzed on the BD FACSVerser flow cytometer with FlowJo software, Version 10. The percentage of maximal binding relative to the highest concentration was graphed and half-maximal effective concentration ( $\text{EC}_{50}$ ) values were determined using GraphPad Prism Version 7.

### **VLS-101 internalization**

To determine whether UC-961 and VLS-101 internalize similarly into cells, experiments were performed on the ROR1<sup>+</sup> MCL cell line, JeKo-1, and on primary cells obtained from CLL patients. For each compound tested,  $7 \times 10^6$  cells were resuspended in 700  $\mu\text{L}$  of cold 2% fetal bovine serum (FBS) in phosphate-buffered saline (PBS). Then 600  $\mu\text{L}$  of this suspension was combined with 600  $\mu\text{L}$  of 60  $\mu\text{g}/\text{mL}$  UC-961 or VLS-101 and incubated on ice for 20 minutes. Cells were washed 5 times with cold 2% FBS in PBS to remove unbound antibody. Cells were then resuspended in 1800  $\mu\text{L}$  of 2% FBS in RPMI. Then 300  $\mu\text{L}$  of antibody were aliquoted into each of 5 tubes for each time point (0, 0.5, 1, 2, and 4 hours). Tubes were placed in a 37°C water bath for the corresponding amount of time. At the end of each time point, cells were stored on ice to stop internalization. Cells were

spun down and incubated in 100  $\mu$ L of anti-human IgG Fc PE (Cat #12499882 Invitrogen used at 1:200) in cold 2% FBS in PBS for 20 minutes on ice in the dark. The remaining 100  $\mu$ L of control cells were also stained as secondary-only controls. Cells were washed 3 times with 2% FBS in PBS, fixed for 10 minutes at room temperature with 2% paraformaldehyde, and then washed again. FACS analysis was done using Miltenyi MACSQuant and BD FlowJo.

### **VLS-101 pharmacokinetics**

Briefly, an immune-affinity approach was used to enrich VLS-101 from mouse plasma using agarose beads coated with Protein A. Because VLS-101 is too large for practical direct quantitative analysis using LC/MS/MS technology, the bound proteins are subjected to “on-bead” enzymatic hydrolysis with papain, releasing the conjugated toxin/drug MMAE. The released MMAE was used as a surrogate for the quantitation of total ADC concentrations.

The VLS-101 dosing schedule of every four days (Q4D) was selected based on the half-life of the total ADC after a single dose in mice. Given that the half-life is  $\sim$  2.5 days, we felt that a Q4D dosing schedule would provide sufficient target coverage.

### **Cell proliferation and in vitro cytotoxicity of VLS-101**

Cells were grown according to ATCC recommendations and were seeded at  $5 \times 10^3$  to  $5 \times 10^4$  per well in a 96-well flat bottom plate with 90  $\mu$ L of growth media per well. A volume of 10  $\mu$ L of pre-diluted VLS-101 (at 10x final concentration), MMAE (at 10x final concentration) or media (control) was added. Three-fold serial dilutions were performed to create 8-point titration curves. For VLS-101, the final concentration range extended from 660 nM to 0.3 nM. For MMAE, the initial concentration range was from 100 nM to 0.015 nM but could be extended to as low as 0.00015 nM. Cells were incubated for 72 hours at 37  $^{\circ}$ C in a carbon dioxide incubator. After 72 hours, proliferation was measured using CellTiter-Glo™ (Promega, PR-G7573). 100  $\mu$ L of CellTiter-Glo™ reagent was added to the 100- $\mu$ L volume of media already present in each well. Contents were

mixed for 15 minutes on an orbital shaker to lyse cells. Luminescence was read on a PerkinElmer EnVision plate reader. Curves and median inhibitory concentration (IC50) values were generated in GraphPad Prism, Version 7, using sigmoidal, dose-response, non-linear regression. The percent inhibition was calculated as:

$$\% \text{ inhibition} = \left( 1 - \left( \frac{\text{Luminescence}_{\text{Inhibitor}} - \text{Luminescence}_{\text{Background}}}{\text{Luminescence}_{\text{PBS}} - \text{Luminescence}_{\text{Background}}} \right) \right) \times 100$$

### **ROR1 expression by immunohistochemistry**

Immunohistochemical (IHC) analysis of ROR1 protein expression was performed at room temperature using the Autostainer Link 48 (Agilent Dako, Carpinteria, CA) with EnVision FLEX reagents (Agilent Dako, Carpinteria, CA). Detection antibodies included anti-human ROR1 mouse monoclonal antibody, OTI3D11 (Origene, Rockville, MD) and a negative control reagent. Pre-sectioned, 4-micron-thick specimens of the tumor were pretreated with antigen retrieval citrate buffer, pH 6.1, at 95-97°C for 40 minutes, rinsed 3 times in distilled water at room temperature, and incubated in wash buffer for 5 minutes. Tissues were placed into the autostainer, washed with wash buffer and incubated with a peroxidase-blocking reagent for 5 minutes. Tissues were then rinsed with wash buffer and incubated with the primary antibody or negative control reagent diluted in an antibody diluent for 60 minutes. Tissues were again rinsed with wash buffer and incubated with a signal-amplifying reagent for 15 minutes. After another wash buffer rinse, tissues were incubated with horseradish peroxidase-conjugated secondary antibody for 20 minutes, followed by a rinse and a 5-minute incubation with wash buffer. Tissues were then incubated with 3,3'-diaminobenzidine (DAB) chromogen for 10 minutes followed by a rinse with wash buffer. Tissues were incubated with hematoxylin for 5 minutes followed by a rinse in distilled water, a 5-minute incubation in wash buffer, and a rinse in distilled water.

Slides were scanned using an Aperio AT Turbo system to produce whole slide images. A 20X JPEG image of each stain is shown. ROR1 expression was evaluated based on a semi-quantitative scale: 0 (unstained), 1+ (weak staining), 2+ (moderate staining), and 3+ (strong staining). An H-score (range of 0 to 300) was calculated using the following equation:  $(3 \times \% \text{ of cells with 3+ staining}) + (2 \times \% \text{ of cells with 2+ staining}) + (1 \times \% \text{ of cells with 1+ staining})$ .

### **ROR1 pathway analysis by western blotting and qRT-PCR**

Total lysates were resolved by SDS-PAGE gels and transferred to nitrocellulose membranes (Bio-Rad, Milan, Italy). The expression of ROR1 and of the relevant molecules of the pathway was confirmed using the following antibodies: ROR1 (#4102), Wnt5a/b (#2530), Rac1/Cdc42 (#4651) and RhoA (#2117) all from Cell Signaling Technologies, Milan, Italy. Bands were detected with an HRP-conjugated anti-rabbit antibody (Santa Cruz Biotechnology). An anti-actin HRP-conjugated antibody was used as a loading control (sc-1616, Santa Cruz Biotechnology). Blots were developed using enhanced chemiluminescence and images acquired with the ImageQuant LAS 4000 ChemiDoc (GE Healthcare). Bands were quantified using the ImageJ free software (<https://imagej.nih.gov/ij/>).

To analyze ROR1 pathway activation, RS cells were incubated with 200 ng/ml recombinant human Wnt5a peptide (#645-WN-010, R&D Systems, Milan, Italy) for different time points at 37 °C. Cells were lysed and proteins resolved as indicated above. Specific antibodies used were P-Jnk (#4671), P-p65 (#3033), P-Akt (#9271) all from Cell Signaling Technologies.

RNA was extracted using RNeasy Plus Mini kit (Qiagen, Milan, Italy) and converted to cDNA using the High Capacity cDNA Reverse Transcription kit (Applied Biosystems). qRT-PCR was performed using the 7900 HT Fast Real Time PCR System (SDS 2.3 software). Primers for *ROR1* (Hs00938677\_m1), *RHOA* (Hs00357608\_m1), *RAC1* (Hs00251654\_m1), *WNT5A* (Hs00998537\_m1), and *B2M* (Hs00984230\_m1) were from Life Technologies. Reactions were done in triplicate from

the same cDNA reaction (technical replicates) and on samples derived from different RS cells obtained from RS-PDXs at different in vivo passages. For each gene, expression levels were computed as a ratio of the number of copies of the target gene over  $10^5$  copies of  $\beta$ -microglobulin (B2M).

### **Immunohistochemistry on RS-PDX models**

For IHC staining, an anti-CD20 antibody (clone L26, #NCL-L-CD20-L26, 1:50, Novocastra) was used to detect RS cells, followed by an anti-mouse HRP-conjugated antibody and 3,3'-diaminobenzidine (EnVision™ System, Dako) to visualize the reaction. Slides were analyzed using an AXIO Lab.A1 microscope (Zeiss), equipped with a Canon EOS600D reflex camera and the images acquired using the ZoomBrowserEX software (Canon).

### **IgH V-J gene sequencing**

DNA from primary RS or RS-PDX purified cells was extracted using a DNA purification kit following manufacturer's instruction (Quiagen, Milan, Italy, #69506). VDJ region was amplified by PCR using specific primers annealing at the 5' L region and at the 3' JH consensus sequence. PCR products were purified with a QIAGEN kit (#28106) and bi-directionally sequenced by Sanger technology using the same PCR primers. Sequences were then analyzed using the IMGT/V-QUEST database <sup>1</sup>.

### **Whole exome sequencing (WES), targeted sequencing and Bioinformatics Analysis**

WES and targeted deep sequencing of RS1050 and IP867/17 were performed as previously described <sup>2</sup>. Briefly, for WES analysis, genomic DNA was sheared and used for the construction of paired end sequencing library. The exome was captured using the SureSelect Human All Exon V6 (Agilent) and sequenced using Illumina Hiseq4000. Genome\_GPS v3.0.2 was used as a comprehensive secondary analysis pipeline for exome sequencing data at Mayo Clinic. For targeted sequencing analysis, genomic DNA purified from RS cells obtained from tumor masses of RS-PDX models was sheared and mutations validated using semiconductor-sequencing technology

(IonTorrent PGM) as per manufacturer's protocol. Targeted deep sequencing was performed on selected twenty-eight genes previously found to be significantly mutated and indicated as putative drivers in CLL. Raw data was aligned and indexed in BAM and BAI files using the IonTorrent suite. Variants were called using IonTorrent Somatic VariantCaller version 4.6.0.7 and low stringency settings (ThermoFisher). VCF files were annotated using BioR. Somatic variants with a Mapping Quality <20 or read depth <10X were removed. Finally, variants of significant interest were visually inspected using Integrative Genomics Viewer (IGV).

Copy Number Variations (CNVs) were called from WES data using a combination of the CNV calling tool PatternCNV (<https://academic.oup.com/bioinformatics/article/30/18/2678/2475632>) and alternative allele frequencies. The four tumor samples IP867\_17\_primary, IP867\_17\_1A, RS1050\_primary, and RS1050\_XaB were run with 46 unrelated samples, that were sequenced with the tumor samples, as a pool of normal. The CNV log<sub>2</sub>ratio from the PatternCNV output was smoothed using the KermSmooth package in R, and used for plotting. The PatternCNV segmentation outputs were used to make final CNV calls. Additionally, alternative allele frequencies of 6,781,919 dbSNP variants were calculated by backfilling reads of the tumor samples using GATK UnifiedGenotyper. Variants from dbSNP with a read depth greater than or equal to 20 were passed for use in plotting. Alternative allele frequencies were used to verify CNV events identified by PatternCNV. CNV log<sub>2</sub>ratio values between tumor and control samples were used to calculate the abnormalities. Log<sub>2</sub>ratio values between -0.5 and 0.5 were considered normal regions; log<sub>2</sub>ratio values < -0.5 were considered deletions; values between 0.5 and 1 were considered one extra copy gain; and log<sub>2</sub>ratio values >1 were classified as 2 or more extra copies.

### **RNA sequencing analysis**

RNA sequencing analysis for RS1316 and RS9737 was performed as previously reported.<sup>2</sup> For RS1050 and IP867/17, approximately 500 ng of total RNA checked for high quality using

Bioanalyzer system (Bioanalyzer RNA 6000 Nano assay, Agilent, Santa Clara, CA), was subjected to the RNA-seq library preparation using TruSeq stranded mRNA Sample Prep Kit (Illumina, San Diego, CA). Samples were sequenced on Illumina NextSeq500 system (NextSeq™ 500/550 High Output Kit v2.5, Illumina) and FastQ data generated. Reads alignment to Homo sapiens UCSC hg19 genome was performed using the RNA-Seq Alignment v2.0.2 tool from Illumina based on the STAR aligner software.<sup>3</sup> An unsupervised analyses was performed computing Z-distribution for each gene based on TPM values to show samples clustering.

### **EBV detection by Fluorescein-Conjugated Epstein-Barr Virus (EBER) staining**

In situ hybridization for EBER was performed on paraffin tissue sections of RS-PDX models using Epstein-Barr Virus RNA (EBER1 and EBER2) PNA Probe/Fluorescein and anti-FITC/AP (EBER RNA CISH; Dako, Denmark) in automatic immunostainer (Omnis).

### **Cell cycle and apoptosis**

RS cells purified from RS-PDX tumor masses were *ex-vivo* exposed to vehicle (PBS) or increasing doses of VLS-101 antibody for different time points. At the end of the treatment, cells were collected and stained with AnnexinV APC-labelled/Propidium Iodide kit or Fix/perm cell cycle kit (ThermoFisher, Milan, Italy) following manufacturer's instructions and samples analyzed by flow cytometry with a BD FACSCanto II/BD FACS Celesta.

Activation of the apoptotic pathway was confirmed by western blotting using an anti-cleaved Caspase-3 (#9662) and an anti-PARP (#9532) antibodies, all from Cell Signaling Technologies (Danvers, MA).

### **Pull-down experiments**

RhoA and Rac1 activation assay reagents were purchased from Cytoskeleton, Inc. (Denver, CO) and used as per the manufacturer's instructions. Briefly, GTP-bound active RhoA or Rac1 was pulled down with Rhotekin-RBD or PAK-PBD beads, respectively, and then subjected to immunoblot

analysis. A negative control (lysate without GTP) and a positive control (lysate incubated with saturating concentration of GTP) were used to assess for non-specific and maximum activation of RhoA or Rac1.

### **Chemotaxis**

The chemotaxis assay across 8.0  $\mu\text{m}$  pore size polycarbonate membranes of a Boyden chamber was performed as described.<sup>4</sup> A total of  $10^5$  cells freshly obtained from tumor masses were seeded in the upper compartment of Transwell inserts. Cells were incubated for 24 hours in 0.5% bovine serum albumin (BSA) medium at 37 °C and 5% CO<sub>2</sub>, and the migration toward chemokine alone (CXCL12, 100 ng/ml or CCL19, 200 ng/ml) or in combination with Wnt5a (400 ng/ml) was analyzed by flow cytometry. The percentage of migrating cells was calculated as the number of migrated cells in response to chemokines divided by the total number of input cells. Experiments were carried out in duplicate, measuring chemotaxis in two separate wells for each condition, for four independent experiments.

### **References**

1. Xochelli A, Agathangelidis A, Kavakiotis I, et al. Immunoglobulin heavy variable (IGHV) genes and alleles: new entities, new names and implications for research and prognostication in chronic lymphocytic leukaemia. *Immunogenetics*. 2015;67(1):61-66.
2. Vaisitti T, Braggio E, Allan JN, et al. Novel Richter Syndrome Xenograft Models to Study Genetic Architecture, Biology, and Therapy Responses. *Cancer Res*. 2018;78(13):3413-3420.
3. Dobin A, Davis CA, Schlesinger F, et al. STAR: ultrafast universal RNA-seq aligner. *Bioinformatics*. 2013;29(1):15-21.
4. Vaisitti T, Aydin S, Rossi D, et al. CD38 increases CXCL12-mediated signals and homing of chronic lymphocytic leukemia cells. *Leukemia*. 2010;24(5):958-969.

## Supplemental Tables

**Supplemental Table 1. Summary of copy-number abnormalities in primary samples and derived RS-PDXs.** CNVs were calculated from WES data. Gain: 1 extra copy; Amplification: 2 or more extra copies.

RS1050_primary		
Genomic coordinates (hg19)	Abnormality	Relevant genes
chr2:38684-50201399	Deletion	
chr2:50246218-54786200	Amplification	
chr2:54826119-56613426	Deletion	
chr2:60983255-65659764	Amplification	<i>REL, XPO1</i>
chr11:197903-134856772	Gain	
chr13:41505945-41910995	Deletion	
chr13:49821937-51858485	Deletion	<i>MIRN15A-MIRN16-1</i>
chr17:5901-21544742	Deletion	<i>TP53</i>
chr17:56393213-81083725	Gain	
chr18:55982991-78005524	Gain	<i>MALT1, TNFRSF11A</i>

RS1050_XaB		
Genomic coordinates (hg19)	Abnormality	Relevant genes
chr2:38684-50201399	Deletion	
chr2:50246218-54786200	Amplification	
chr2:54826119-56613426	Deletion	
chr2:60983255-65659764	Amplification	<i>REL, XPO1</i>
chr6:203289-14118464	Gain	
chr6:14131565-32610906	Deletion	
chr10:92718-135473215	Gain	
chr11:192925-134856772	Gain	
chr13:41505945-41910995	Deletion	
chr13:49821937-51858485	Deletion	<i>MIRN15A-MIRN16-1</i>
chr17:5901-21912207	Deletion	<i>TP53</i>
chr18:55915957-78005524	Gain	<i>MALT1, TNFRSF11A</i>

IP867_primary		
Genomic coordinates (hg19)	Abnormality	Relevant genes
chr6:32709036-33769112	Deletion	
chr6:92231177-101338488	Deletion	
chr6:105175830-105245013	Deletion	
chr6:111588724-126301494	Deletion	
chr6:129511231-170893906	Deletion	
chr7:192859-5461288	Gain	
chr7:6590529-35675194	Deletion	
chr7:46728156-65619662	Deletion	
chr8:75460668-124526695	Gain	
chr8:124543928-124710968	Amplification	
chr8:124714772-127569857	Gain	
chr8:128097983-128753826	Amplification	<i>MYC</i>
chr8:128808025-146281522	Gain	
chr13:61988962-90883635	Deletion	
chr13:94938416-115092914	Deletion	
chr14:19553255-107283249	Deletion	
chr15:20169887-102389910	Deletion	
chr17:5901-17942695	Deletion	<i>TP53</i>
chr17:75392954-81083725	Gain	

IP867_1A		
Genomic coordinates (hg19)	Abnormality	Relevant genes
chr3:11401945-59035853	Deletion	
chr4:53069-190904008	Deletion	
chr8:162890-75279436	Deletion	
chr8:82741506-89340407	Deletion	
chr8:109795236-113421424	Deletion	
chr8:121237217-124351788	Deletion	
chr8:124543928-124710968	Amplification	
chr8:124714772-127569857	Deletion	
chr8:128097983-128753826	Amplification	<i>MYC</i>
chr8:128808025-131964385	Deletion	
chr9:40498370-141069431	Deletion	
chr11:119043400-132182756	Deletion	
chr12:175827-133812807	Deletion	
chr13:30776657-39624353	Deletion	
chr13:51590915-93879973	Deletion	
chr13:103392228-107863211	Deletion	
chr14:19553255-107283249	Deletion	
chr15:20169887-102389910	Deletion	
chr17:5901-17943326	Deletion	<i>TP53</i>

**Supplemental Table 2. IgVH mutational status of RS-PDX models**

Model identification	IgVH	% of IgVH mutations
IP867/17 Primary	IGHV3-49*04; IGHJ6*02	2.7
IP867/17 PDX	IGHV3-49*04; IGHJ6*02	2.7
RS1316 Primary	IGHV3-21*01; IGHJ3*02	0
RS1316 PDX	IGHV3-21*01; IGHJ3*02	0
RS1050 Primary	IGHV4-34*02; IGHJ4*02	2.1
RS1050 PDX	IGHV4-34*02; IGHJ4*02	2.1
RS9737 Primary	IGHV3-7*01; IGHJ4*02	1.01
RS9737 PDX	IGHV3-7*01; IGHJ4*02	1.01

IgVH usage and percentage of mutation of the 4 RS-PDXs available and employed in the study.

**Supplemental Table 3. Mutational profile of the RS-PDX models.** Mutations found by whole-exome sequencing (WES) or targeted sequencing in the RS-PDX models used in the study. Frequencies of mutation are reported by color-coding, as indicated. Variants already present in primary samples are depicted with a box with a central dot. VAF: variant allele frequency; SAV: splice-site variant; del: deletion; fs: frameshift.

RS-PDXs	IP867/17	RS1316	RS1050	RS9737
<b>Gene ID and mutation</b>				
<i>TP53</i> (c.673-2A>G; SAV)			•	
<i>TP53</i> (c.254delC; fs)	•			
<i>TP53</i> (p.H214fs)				•
<i>NOTCH1</i> (p.2514fs4)				•
<i>NOTCH2</i> (p.N1516S)		•		
<i>BTK</i> (p.E96G)				•
<i>BTK</i> (p.C481S)		•		
<i>MYC</i> (p.P60T)		•		
<i>PIK3C2G</i> (c.3263delA; fs)		•		
<i>KRAS</i> (p.G13C)		•		
<i>KRAS</i> (p.L19F)				•
<i>KRAS</i> (p.T58I)				•
<i>EGR2</i> (p.H384N)			•	•
<i>EGR2</i> (p.D411Y)				•
<i>SETD2</i> (p.G889V)				•
<i>TRAF3</i> (c.1230_1231delGA; fs)	•			
<i>TRAF3</i> (p.T411S)	•			
<i>MED12</i> (p.G44R)		•		
<i>TBL1XR1</i> (p.H127p)		•		
<i>ERBB3</i> (p.V606I)			•	
<i>CYLD</i> (p.L475F)			•	
<i>SMAD5</i> (p.S351T)			•	
<i>PTPRK</i> (p.W1055L)			•	
<i>PAX5</i> (p.K196M)			•	
<i>VCAM1</i> (p.P254A)			•	
<i>STAT3</i> (p.K283T)			•	
<i>NFKBIZ</i> (p.L399P)			•	

•	$0 \leq \text{VAF} \leq 0.30$
•	$0.31 \leq \text{VAF} \leq 0.60$
•	$0.61 \leq \text{VAF} \leq 1.00$

•	Variants already present in the primary sample
•	
•	

**Supplemental Table 4. VLS-101 pharmacokinetics.** Pharmacokinetics data of VLS-101 administered at 2 and 5 mg/kg resulted in a maximum plasmatic concentration (C<sub>max</sub>) of 29.6 and 73.8 µg/ml, respectively. AUC<sub>INF</sub>: area under the curve; t<sub>1/2</sub>: half-life.

VLS-101	C <sub>max</sub> (µg/mL)	AUC <sub>INF</sub> (h*µg/mL)	t <sub>1/2</sub> (h)
2 mg/kg	29.6	1690	58.8
5 mg/kg	73.8	2520	57.6

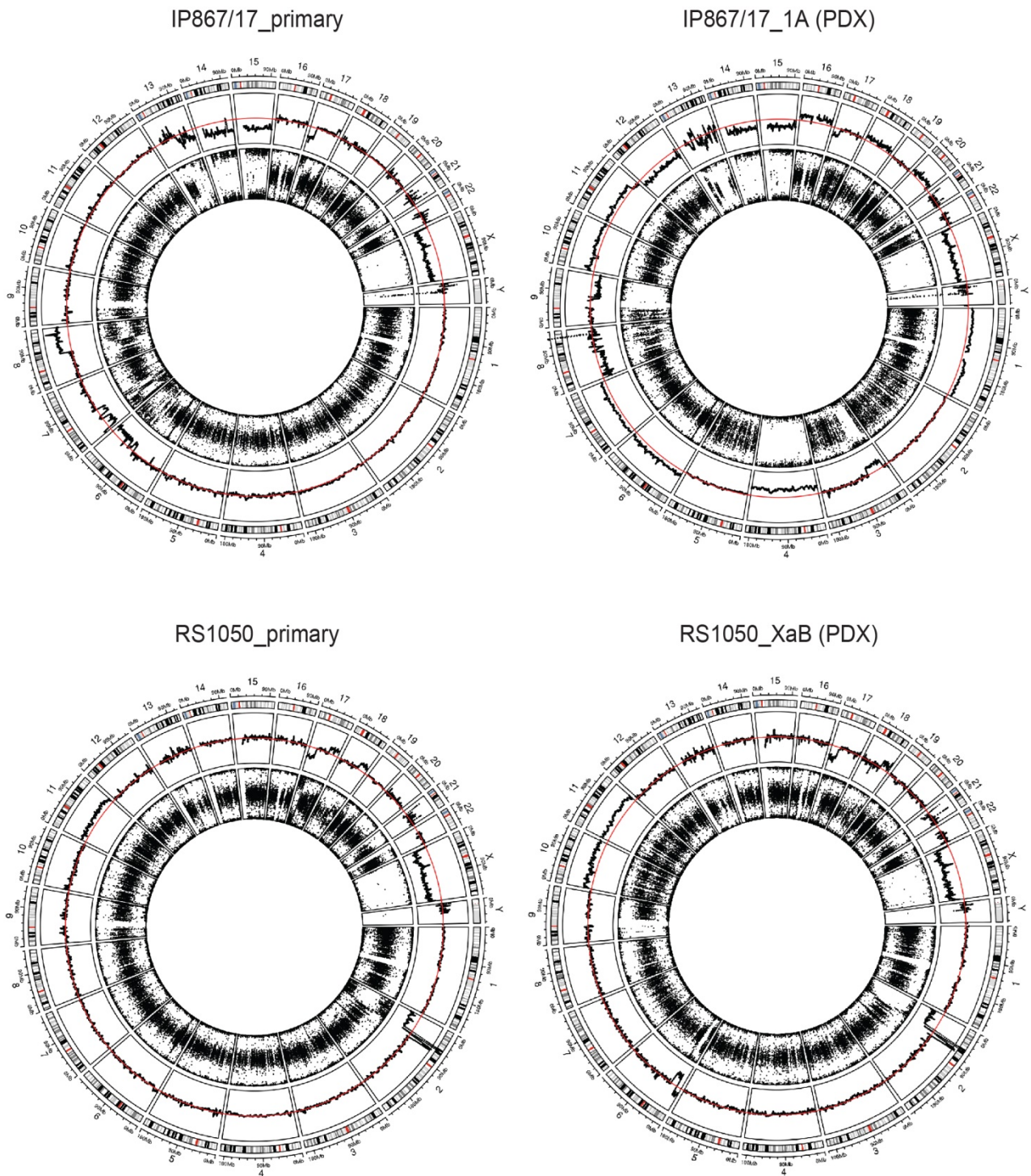
**Supplemental Table 5. In vitro cytotoxicity of VLS-101.** Data showing the IC<sub>50</sub> of VLS-101 assessed in different cell lines.

<sup>a</sup>. Cell viability after 72 hours of incubation with VLS-101, as assessed by CellTiter-Glo™; average of ≥2 experiments. MCL=mantle cell lymphoma; DLBCL=diffuse large B-cell lymphoma; IC<sub>50</sub>=half-maximal inhibitory concentration.

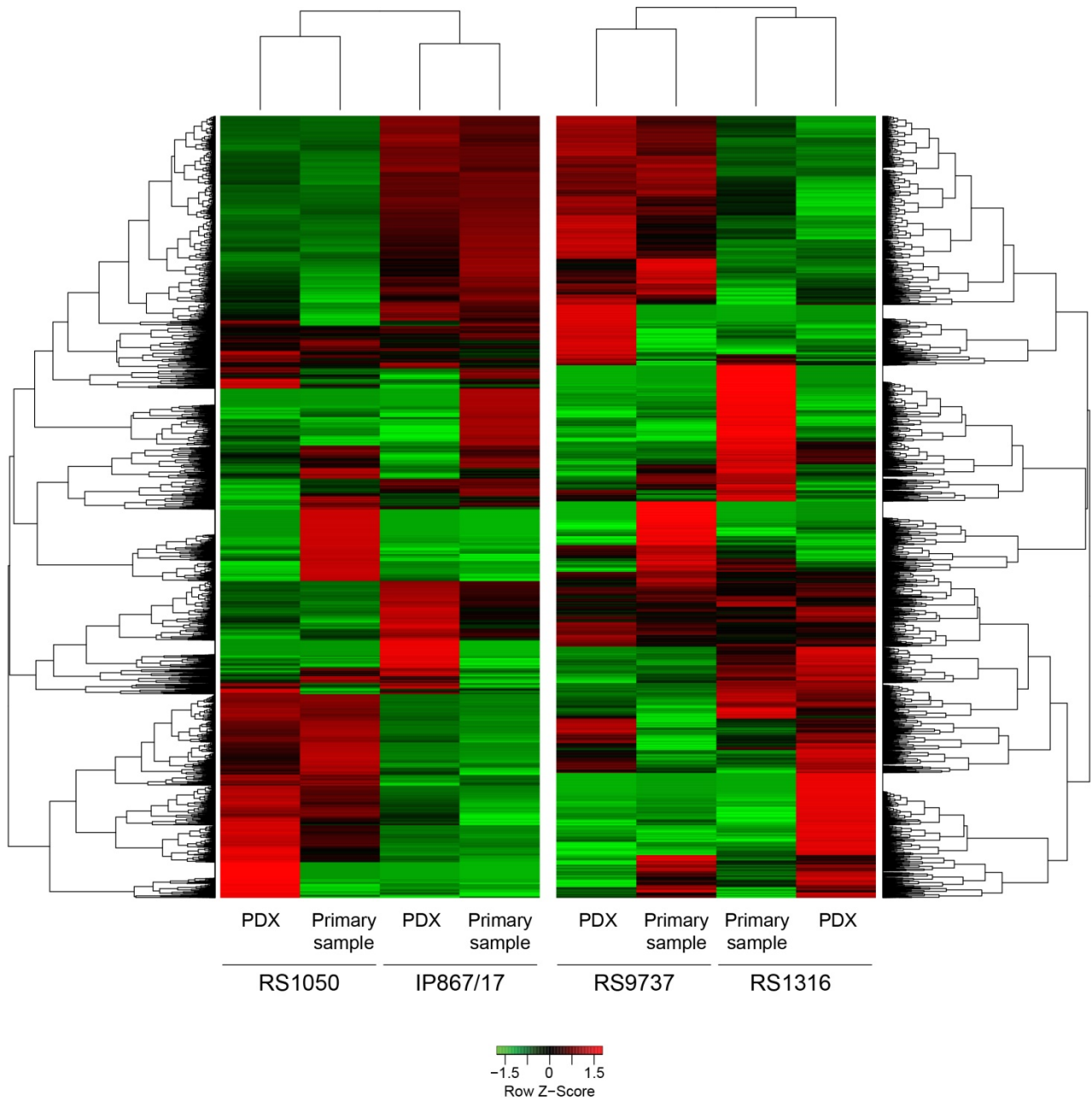
Cell Line	Cancer Type	VLS-101 IC <sub>50</sub> , µg/ml <sup>a</sup>
JeKo-1	MCL	28.3
Mino	MCL	3.0
OCI-Ly18	DLBCL	14.4
HBL-1	DLBCL	12.9
DOHH2	DLBCL	19.5
WSU-DLCL	DLBCL	10.3

## Supplemental Figures

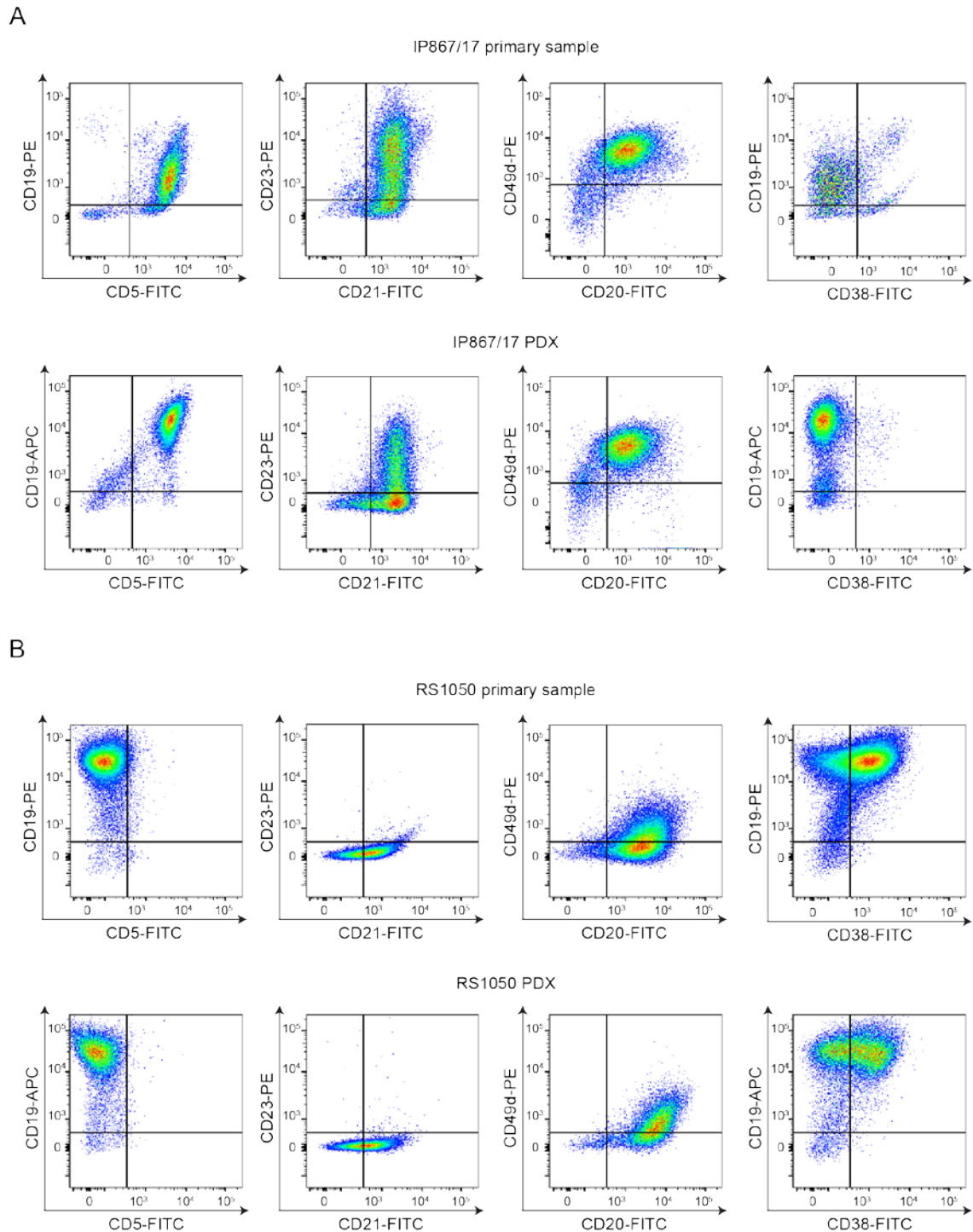
**Supplemental Figure 1. Genomic profile of primary and corresponding PDX.** Circos plots showing the copy number abnormalities (CNVs) for primary sample and the corresponding PDX. In each plot the outer and inner graphs represent the CNV log<sub>2</sub>ratio values and the alternative allele frequencies, respectively.



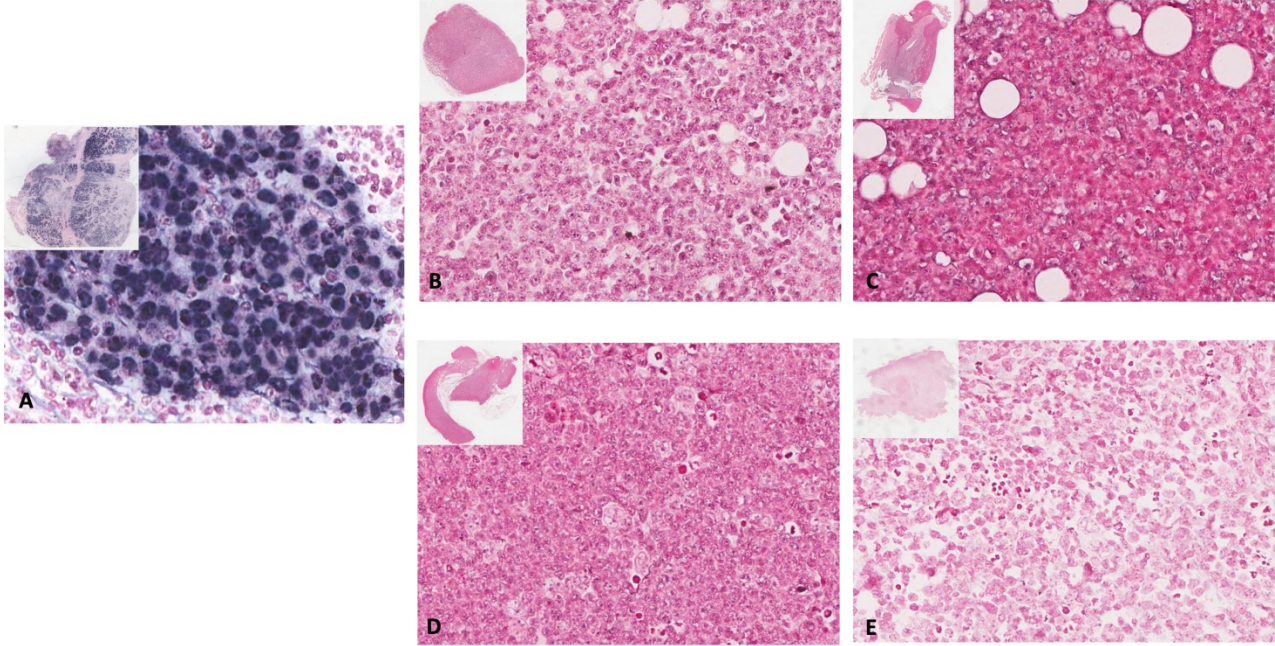
**Supplemental Figure 2. Transcriptomic profile of primary and PDX models.** Unsupervised analysis of RNA sequencing data of primary RS cells and their corresponding PDXs. Data showed that each PDX model clusters together with its primary sample, highlighting that most of the transcriptomic profile is maintained.



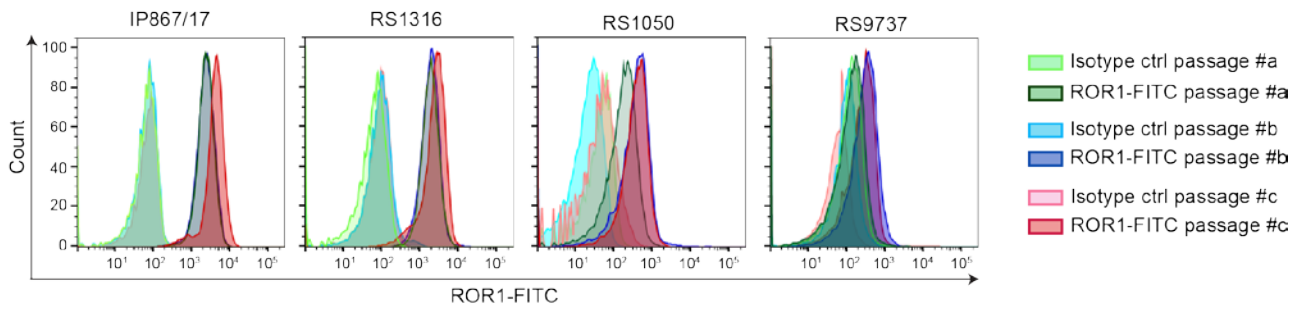
**Supplemental Figure 3. Immunophenotype of primary and RS-PDX-derived cells of the IP867/17 and RS1050 models.** RS cells obtained from the patient (primary sample) and from the respective PDX were stained for different surface molecules (CD19; CD5; CD21; CD23; CD20; CD49d; CD38) using anti-human specific antibodies and analyzed by flow cytometry.



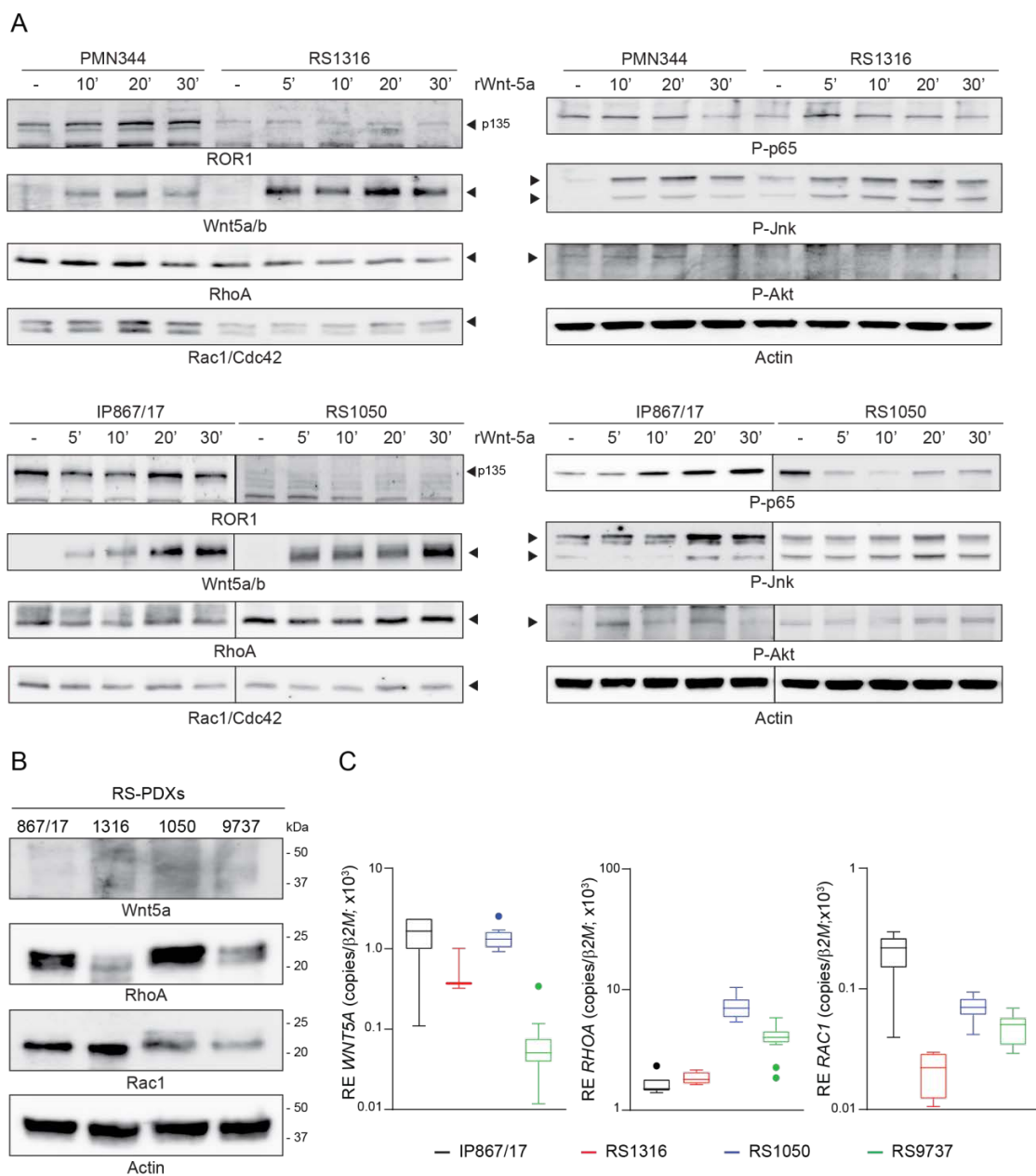
**Supplemental Figure 4. EBV detection on PDX models.** Analysis of EBV infection by EBER test on tumor masses from the 4 RS-PDX models used in this study. Oropharyngeal squamous cell carcinoma was used as positive control (A). RS9737 (B); RS1316 (C); IP867/17 (D); RS1050 (E). Original magnification x400; insets x7.



**Supplemental Figure 5. ROR1 expression on RS-PDX models is stable over-time.** Cell surface expression of ROR1 on RS cells obtained from PDXs at different in vivo passages detected by flow cytometry using an anti-ROR1 FITC-conjugated antibody. An isotype antibody was used as control. Three different passages are depicted in each plot.

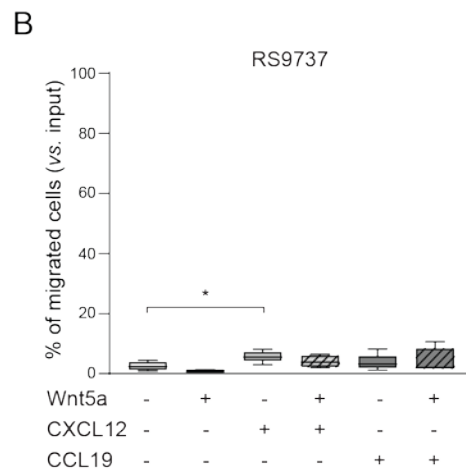
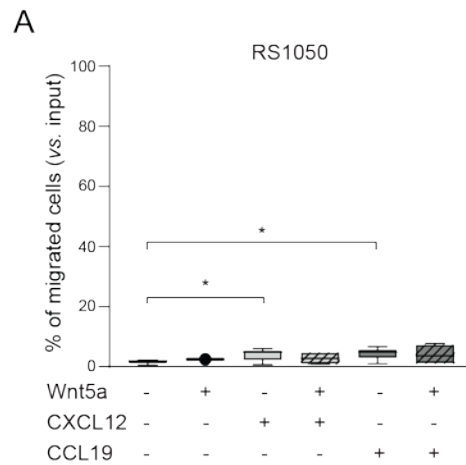


**Supplemental Figure 6. Signaling cascade and expression of ROR1 downstream elements in RS-PDX models.** ROR1 signaling cascade was analyzed in ROR1-expressing RS-PDX models following exposure to recombinant Wnt5a (200 ng/ml) for different time points. A CLL patient (PMN344) was included as control. Expression and phosphorylation of several targets was analyzed (A). Western blots (B) and qRT-PCR (C) data showing the expression ROR1 ligand Wnt5a, RhoA and Rac1, two key players of ROR1 signaling pathway. Actin was used as a loading control in western blot. qRT-PCR data (from at least 4 different tumor masses) are reported as relative expression (RE) of the target gene over b-2-microglobulin. Box plots show the distribution of values: median, interquartile range, min and max values (Tukey representation).

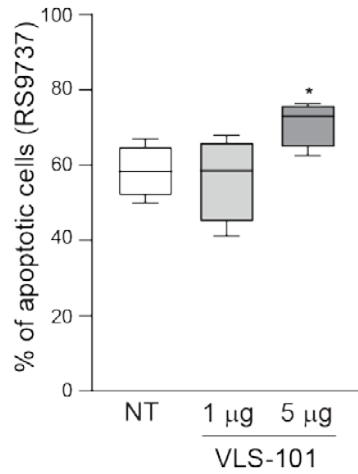


**Supplemental Figure 7. RS cells chemotaxis.** Chemotaxis in response to CXCL12 and CCL19, alone or in combination with Wnt5a, of RS1050 (A) and RS9737 (B) cells purified from RS-PDX tumor masses (5 and 4 independent experiments, respectively). Migration is plotted as % of migrating cells calculated as [number of cells in the lower chamber/(number of cells in the upper chamber + number of cells in the lower chamber)]\*100.

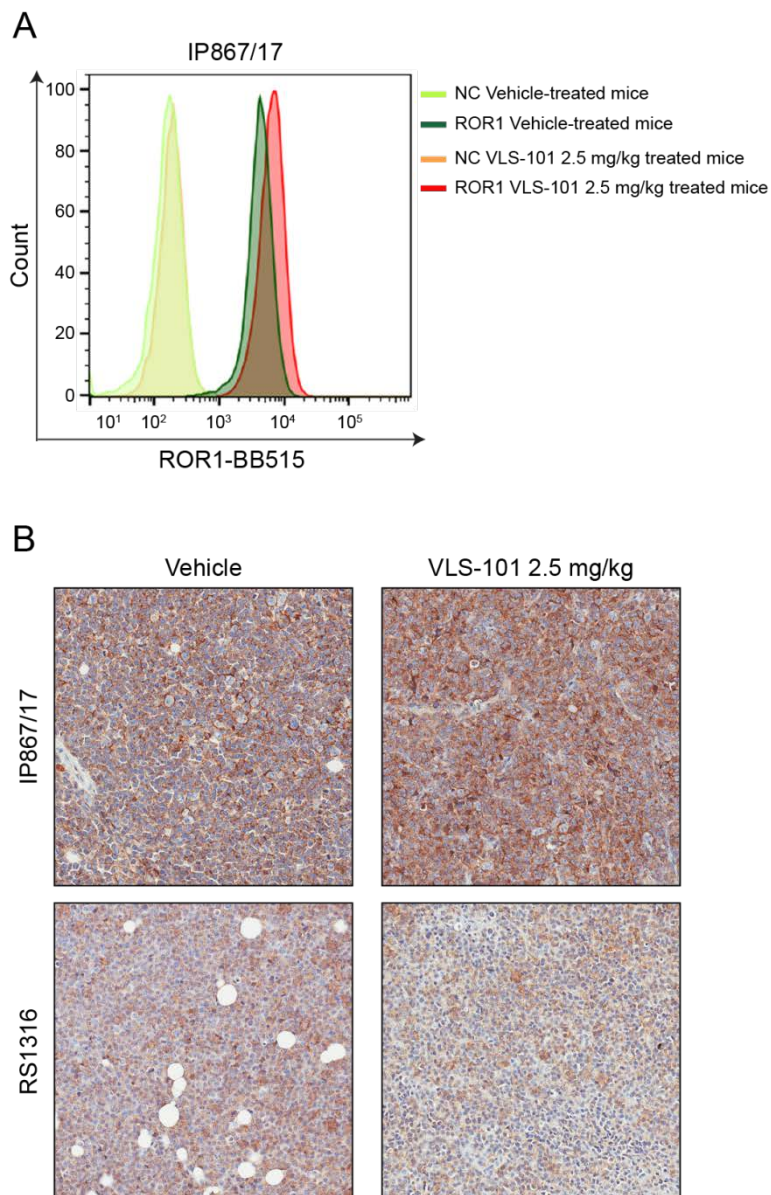
Statistical analysis was performed using the Mann-Whitney test. Box plots show the distribution of values: median, interquartile range, min and max values. \* p<0.05



**Supplemental Figure 8. Ex vivo apoptosis of ROR1<sup>-</sup> RS cells.** RS9737 cells purified from tumor masses (4 independent experiments) were incubated with the indicated doses of VLS-101, stained with AnnexinV/propidium iodide and analyzed for apoptosis by flow cytometry. Box plots show the distribution of values: median, interquartile range, min and max values. Statistical analyses were performed using paired t-test. NT: untreated cells. \* p<0.05



**Supplemental Figure 9. ROR1 expression on RS cells after VLS-101 treatment.** ROR1 expression evaluated by flow cytometry (A) and IHC (B) on RS cells obtained from tumor masses regrown after VLS-101 treatment (mice were treated as indicated in Figure 6) in s.c. RS-PDXs. After treatment, mice were monitored for tumor re-growth. When masses reached the maximum volume, mice were euthanized, and tumor masses collected, partially dismantled to obtain a single cell suspension (for flow data) and partially formalin-fixed and paraffin embedded (for IHC analysis). Slides were scanned using an Aperio AT Turbo system to produce whole slide images. A 20X JPEG image of each stain is shown. NC: negative control.



**Supplemental Figure 10. Correlation between mRNA levels and surface expression of ROR1 in RS cells.** Correlation between mRNA levels of ROR1 expression measured by RT-PCR (number of copies over beta-2-microglobulin; log scale) and its surface expression analyzed by flow cytometry (% of ROR1<sup>+</sup> cells). RS-PDX models characterized by the highest mRNA levels (IP867/17 and RS1316) are the ones showing the higher expression of ROR1 by flow cytometry. RS cells were obtained from tumor masses. A Pearson correlation was calculated ( $r=0.8878$ ;  $p\text{ value}<0.0001$ ).

